arXiv:1609.02891v1 [cond-mat.stat-mech] 9 Sep 2016

Stable and accurate schemes for Langevin dynamics with general kinetic energies

Gabriel Stoltz[1] and Zofia Trstanova[2]
[1] Université Paris-Est, CERMICS (ENPC), INRIA, F-77455 Marne-la-Vallée, France
[2] Univ. Grenoble Alpes, LJK, INRIA, F-38000 Grenoble, France

September 12, 2016

Abstract

We study Langevin dynamics with a kinetic energy different from the standard, quadratic one in order to accelerate the sampling of the Boltzmann–Gibbs distribution. We consider two cases: kinetic energies which are local perturbations of the standard kinetic energy around the origin, where they vanish (this corresponds to the so-called adaptively restrained Langevin dynamics); and more general non-globally Lipschitz energies. We develop numerical schemes which are stable and of weak order two, by considering splitting strategies where the discretizations of the fluctuation/dissipation are corrected by a Metropolis procedure. We use the newly developped schemes for two applications: optimizing the shape of the kinetic energy for the adaptively restrained Langevin dynamics, and reducing the metastability of some toy models with non-globally Lipschitz kinetic energies.

1 Introduction

In statistical physics, the macroscopic information of interest for the systems under consideration can be inferred from averages over microscopic configurations distributed according to probability measures μ characterizing the thermodynamic state of the system [3, 28]. Due to the high dimensionality of the system (which is proportional to the number of particles), these configurations are most often sampled using trajectories of stochastic differential equations or Markov chains ergodic for the probability measure μ; see for instance [15, 18].

We focus here on a typical choice for μ, namely the Boltzmann–Gibbs measure, which describes a system at constant temperature. One popular stochastic process allowing to sample this measure is the Langevin dynamics. We denote the configuration of the system by $(q,p) \in \mathcal{E}$, where $q \in \mathcal{D}^d$ are the positions of the particles in the system (with $\mathcal{D} = \mathbb{R}$ or $\mathcal{D} = \mathbb{R}/\mathbb{Z}$ for systems with periodic boundary conditions), and $p \in \mathbb{R}^d$ the associated momenta. For general separable Hamiltonian energies of the form $H(q,p) = V(q)+U(p)$, the Langevin dynamics reads

$$\left\{ \begin{array}{l} dq_t = \nabla U(p_t)\, dt, \\ dp_t = -\nabla V(q_t)\, dt - \gamma \nabla U(p_t)\, dt + \sqrt{\dfrac{2\gamma}{\beta}}\, dW_t, \end{array} \right. \tag{1}$$

where dW_t is a standard d-dimensional Wiener process, β is proportional to the inverse temperature and $\gamma > 0$ is the friction constant. The corresponding Boltzmann–Gibbs (or canonical) measure is

$$\mu(dq\, dp) = Z_\mu^{-1} \mathrm{e}^{-\beta H(q,p)}\, dp\, dq, \qquad Z_\mu = \int_{\mathcal{E}} \mathrm{e}^{-\beta H(q,p)}\, dp\, dq. \tag{2}$$

Averages of an observable φ with respect to this distribution are approximated by ergodic averages as

$$\lim_{t\to\infty} \widehat{\varphi}_t = \mathbb{E}_\mu(\varphi) \quad \text{a.s.}, \qquad \widehat{\varphi}_t := \frac{1}{t}\int_0^t \varphi(q_s, p_s)\, ds. \tag{3}$$

In practice, the Langevin dynamics (1) cannot be analytically integrated. Its solution is therefore approximated with a numerical scheme. The numerical analysis of such discretization schemes is by now well-understood when U is the standard quadratic kinetic energy. We refer for instance to [19, 14] for implicit schemes suited for dynamics in unbounded spaces, and to [6, 7, 16, 1] for mathematical studies of the properties of splitting schemes.

One important limitation of the estimators $\widehat{\varphi}_t$ in (3) are their possibly large statistical errors. Under certain assumptions on U, V (see *e.g.* [18, 22] and references therein), it can be shown that a central limit theorem holds true, so that $\sqrt{t}[\widehat{\varphi}_t - \mathbb{E}_\mu(\varphi)]$ converges in law to a centered Gaussian distribution of variance σ_φ^2. The asymptotic variance σ_φ^2 may be large due to the metastability of the Langevin process, which occurs as soon as the probability measure μ is multimodal (*i.e.* it has modes of large probabilities separated by low-probability regions). Since the statistical error scales as $\sigma_\varphi/\sqrt{t}$, there are three ways to decrease it *at fixed computational time*:

(i) decrease the value of the asymptotic variance σ_φ by using variance reduction techniques (stratification, importance sampling, control variates, etc; see for instance the review in [18, Section 3.4]);

(ii) increase the timestep Δt in order to increase the simulated physical time $N_{\text{iter}}\Delta t$ at fixed number of iterations. The most important limitations on Δt are related to the stability of the schemes under consideration;

(iii) decrease the computation cost of a single step in order to increase the number of iterations N_{iter}.

In this work, we consider the discretization of modified Langevin dynamics which improve the sampling of the Boltzmann–Gibbs distribution by introducing a more general kinetic energy function U than the standard quadratic one. Stability is our main concern in this work, although we also discuss some importance sampling strategy in Section 5. We have in fact two situations in mind:

(a) adaptively restrained Langevin dynamics [2], where the kinetic energy vanishes for small momenta, while it agrees with the standard kinetic energy for large momenta. The interest of this dynamics is that slow particles are frozen. The computational gain follows from the fact that the interactions between frozen particles need not be updated. A mathematical analysis of the asymptotic variance for this method is presented in [22], while the algorithmic speed-up, which allows to decrease the cost of a single iteration, is made precise in [27];

(b) Langevin dynamics with kinetic energies growing more than quadratically at infinity, in an attempt to reduce metastability. Recall indeed that the crucial part of the sampling of the canonical measure is the position marginal $\nu(dq) = Z_\nu^{-1}\mathrm{e}^{-\beta V(q)}\, dq$. The marginal distribution of μ in the variable q is always ν, whatever the choice of the kinetic energy U. The extra freedom provided by U can be used in order to reduce the metastability of the dynamics when the aim is to sample μ.

The main issue with the situations we consider is the stability of discretized schemes. Several works indicate that explicit discretizations of Langevin-type dynamics with non-globally Lipschitz force fields are often unstable (in the sense that the corresponding Markov chains do not admit invariant measures), see *e.g.* [19]. We face such situations here, even for compact position spaces, when ∇U is not globally Lipschitz. For adaptively restrained Langevin dynamics, the difficulties arise from the possibly abrupt transition from the region where the kinetic energy

vanishes to the region where it coincides with the standard one. Numerical evidence reported in [27] indicate that such a fast transition provides a favorable trade-off between the reduced algorithmic complexity and the increase in the asymptotic variance. Abrupt transitions however lead to large "kinetic" forces $\nabla U(p)$ in some regions and hence limit admissible timesteps. As for the stabilization of the Euler-Maruyama discretization of overdamped Langevin dynamics in [23], we suggest to use a Metropolis acceptance/rejection step [20, 13] in order to ensure the stability of the methods under consideration. Such a stabilization leads to schemes which can be seen as one step Hybrid Monte Carlo (HMC)[1] algorithms [8] with partial refreshment of the momenta, studied for instance in [7] for the standard kinetic energy. Here, in order to obtain a weakly consistent method of order 2 (which is no longer trivial when the fluctuation/dissipation cannot be analytically integrated), we rely on the Metropolis schemes developed for overdamped Langevin dynamics in [9].

This article is organized as follows. In Section 2, we recall the modified Langevin dynamics and possible strategies for its discretization. We next describe in Section 3 the generalized Hybrid Monte Carlo scheme we consider, and prove that it is weakly consistent of order 2. We next turn to numerical results relying on the stability properties of the Metropolized scheme. We first propose, for the adaptively restrained Langevin, a better kinetic energy function than the one originally suggested in [2] (see Section 4). We finally demonstrate on a simple example how the choice of non-quadratic kinetic energies can dramatically improve the sampling efficiency (see Section 5).

2 Discretization of Langevin dynamics

We consider in all this work kinetic energies U and potentials V which are smooth functions growing at most polynomially at infinity and such that

$$\int_{\mathbb{R}^d} \mathrm{e}^{-\beta U} < +\infty, \qquad \int_{\mathcal{D}^d} \mathrm{e}^{-\beta V} < +\infty.$$

We denote by

$$\mathcal{L} = \mathcal{L}_{\rm Ham} + \mathcal{L}_{\rm FD}, \qquad \mathcal{L}_{\rm Ham} = \nabla U \cdot \nabla_q - \nabla V \cdot \nabla_p, \qquad \mathcal{L}_{\rm FD} = \gamma \left(-\nabla U \cdot \nabla_p + \frac{1}{\beta} \Delta_p \right), \quad (4)$$

the generator of the dynamics (1). A simple computation shows that (1) leaves the measure (2) invariant since, for all C^∞ functions φ with compact support,

$$\int_{\mathcal{E}} \mathcal{L}\varphi \; d\mu = 0.$$

We refer for instance to the review in [18] for convergence results for the Langevin dynamics associated with the standard kinetic energy

$$U_{\rm std}(p) = \frac{1}{2} p^T M^{-1} p, \quad (5)$$

where M is a positive mass matrix (typically a diagonal matrix, where the entries are the inverses of the masses of the particles in the system). These convergence results are stated either in terms of ergodic averages (Law of Large Numbers and Central Limit Theorem) or in terms of the law of the process at time t.

For a given timestep $\Delta t > 0$, numerical schemes approximate the solution $(q_{n\Delta t}, p_{n\Delta t})$ of the Langevin dynamics (1) by (q^n, p^n). The sequence $(q^n, p^n)_{n \geqslant 0}$ usually is a Markov chain.

[1] Also called "Hamiltonian Monte-Carlo" in the statistics community.

One appealing strategy to construct numerical schemes for Langevin dynamics is to resort to a splitting scheme between the Hamiltonian part of the dynamics (typically integrated with a Verlet scheme [29]) and the fluctuation/dissipation dynamics on the momenta. The corresponding dynamics

$$dp_t = -\gamma \nabla U(p_t)\, dt + \sqrt{\frac{2\gamma}{\beta}}\, dW_t, \tag{6}$$

with generator $\mathcal{L}_{\rm FD}$, cannot be analytically integrated, except for very specific kinetic energies such as $U_{\rm std}$ defined in (5). However, a simple extension of the results of [16] shows that splitting schemes (either Lie or Strang) based on a weakly second order consistent discretization of (6) and a Verlet scheme for the Hamiltonian part are globally weakly consistent, of weak order 1 for Lie-based splittings and of weak order 2 for Strang based splittings. Moreover, in the case when the kinetic energy is a perturbation of the standard kinetic energy, in the sense that

$$\|\nabla U - \nabla U_{\rm std}\|_{L^\infty} < +\infty, \tag{7}$$

it can be shown that the numerical schemes admit a unique invariant probability measure $\mu_{\Delta t}$. Moreover, it is possible to prove exponential convergence in some weighted L^∞ spaces, with rates which are uniform in the timestep Δt and depend only on the physically elapsed time. This allows also to state error estimates on the invariant measure $\mu_{\Delta t}$ and on integrated correlation functions. Such results are obtained by adapting the proofs of the corresponding statements in [16], upon replacing $\nabla U_{\rm std}(p) = M^{-1}p$ with $\nabla U(p) = M^{-1}p + Z(p)$ where Z is uniformly bounded (see [26]).

On the other hand, when the condition (7) is not satisfied, it may not be possible to prove the existence of a unique invariant measure for the splitting schemes. The main obstruction is that the Markov chain corresponding to the discretization of the elementary fluctuation/dissipation dynamics (6) may itself be transient. This would be the case for instance for non-globally Lipschitz force fields ∇U and a Euler-Maruyama discretization [23]. This observation motivates resorting to a Metropolis correction in order to ensure the existence of an invariant probability distribution.

3 Generalized Hybrid Monte-Carlo schemes

We present in this section a generalized Hybrid Monte-Carlo (GHMC) scheme to discretize the Langevin dynamics with non-quadratic kinetic energies. For an introduction to HMC and some of its generalizations, we refer for instance the reader to [17, Section 2.2.3]. In essence, HMC is a Metropolis-Hastings method based on a proposal generated by the integration of the deterministic Hamiltonian dynamics. The proposal is then accepted or rejected according to the Metropolis rule. The rejection of the proposal occurs due to discretization errors. The efficiency of the method is therefore a trade-off between larger simulated physical times (which calls for larger timesteps) and not too large rejection rates (which places an upper limit on possible timesteps).

We metropolize the Langevin dynamics with a general kinetic energy in two steps: first, we metropolize the Hamiltonian part as in the standard single-step HMC method (see Section 3.1); in a second step, we add a weakly consistent discretization of the elementary fluctuation/dissipation stabilized by a Metropolis procedure (see Section 3.2). The complete algorithm is summarized in Section 3.3.

In order to state rigorous results, we work with functions growing at most polynomially. More precisely, introducing the weight function $\mathcal{K}_\alpha(q,p) = 1 + |q|^\alpha + |p|^\alpha$, we consider the following spaces of functions growing at most as $\mathcal{K}_\alpha$ at infinity:

$$L^\infty_{\mathcal{K}_\alpha} = \left\{ f \text{ measurable}, \quad \|f\|_{L^\infty_{\mathcal{K}_\alpha}} = \left\| \frac{f}{\mathcal{K}_\alpha} \right\|_{L^\infty} < +\infty \right\}.$$

In order to write more concise statements, we will simply say that a sequence of functions $f_{\Delta t}$ grows at most polynomially in (q,p) uniformly in Δt when there exist $K, \alpha, \Delta t^* > 0$ such that

$$\sup_{0<\Delta t\leqslant \Delta t^*} \|f_{\Delta t}\|_{L^\infty_{\mathcal{K}_\alpha}} \leqslant K. \tag{8}$$

We finally define the vector space $\mathscr{S}$ of smooth functions which, together with all their derivatives, grow at most polynomially.

3.1 Metropolization of the Hamiltonian part

Let us describe the one-step HMC method we use to discretize the Hamiltonian part of the dynamics:

$$\begin{cases} dq_t = \nabla U(p_t)\, dt, \\ dp_t = -\nabla V(q_t)\, dt. \end{cases} \tag{9}$$

Starting from a configuration $(q^n, p^n) \in \mathcal{E}$, a new configuration $(\widetilde{q}^{n+1}, \widetilde{p}^{n+1}) = \Phi_{\Delta t}(q^n, p^n) \in \mathcal{E}$ is proposed using the Verlet scheme

$$\begin{cases} p^{n+1/2} = p^n - \nabla V(q^n)\dfrac{\Delta t}{2}, \\ \widetilde{q}^{n+1} = q^n + \nabla U(p^{n+1/2})\Delta t, \\ \widetilde{p}^{n+1} = p^{n+1/2} - \nabla V(\widetilde{q}^{n+1})\dfrac{\Delta t}{2}. \end{cases} \tag{10}$$

The proposal is then accepted with probability

$$A^{\mathrm{Ham}}_{\Delta t}\left(q^n, p^n\right) = \min\left(1, \exp\left(-\beta\Big[H\left(\Phi_{\Delta t}(q^n,p^n)\right) - H\left(q^n,p^n\right)\Big]\right)\right). \tag{11}$$

If the proposal is rejected, a momentum reversal is performed and the next configuration is set to $(q^{n+1}, p^{n+1}) = (q^n, -p^n)$ (see the discussion in [17, Section 2.2.3] for a motivation of the momentum reversal). In summary, the new configuration is

$$\begin{aligned} \left(q^{n+1}, p^{n+1}\right) &= \Psi^{\mathrm{Ham}}_{\Delta t}(q^n, p^n, \mathcal{U}^n) \\ &= \mathbb{1}_{\left\{\mathcal{U}^n \leqslant A^{\mathrm{Ham}}_{\Delta t}(q^n,p^n)\right\}} \Phi_{\Delta t}\left(q^n, p^n\right) + \mathbb{1}_{\left\{\mathcal{U}^n > A^{\mathrm{Ham}}_{\Delta t}(q^n,p^n)\right\}} \left(q^n, -p^n\right), \end{aligned} \tag{12}$$

where $(\mathcal{U}^n)_{n\geqslant 0}$ is a sequence of independent and identically distributed (i.i.d.) random variables uniformly distributed in $[0,1]$. A simple proof shows that the canonical measure μ is invariant by the scheme (12). The corresponding Markov chain is however of course not ergodic with respect to μ since momenta are not resampled or randomly modified at this stage (this will be done by the discretization of the fluctuation/dissipation, see Section 3.3 for the complete GHMC scheme).

Without any discretization error (*i.e.* if the Hamiltonian dynamics was exactly integrated, so that the energy would be constant), the proposal would always be accepted. Since the Verlet scheme is of order 2, we expect the energy difference $H\left(\Phi_{\Delta t}(q^n,p^n)\right) - H\left(q^n,p^n\right)$ to be of order Δt^3. The following lemma makes this intuition rigorous and quantifies the canonical average of the rejection rate $1 - A^{\mathrm{Ham}}_{\Delta t}$ in terms of the timestep Δt and derivatives of the potential and kinetic energy functions.

Lemma 3.1. *Assume that $U, V \in \mathscr{S}$ and that the canonical measure μ admits moments of all order in q, p. Then there exist $K, \Delta t^*, \alpha > 0$ such that the rejection rate of the one-step HMC scheme* (12) *admits the following expansion: for any $\Delta t \in (0, \Delta t^*]$,*

$$0 \leqslant 1 - A^{\mathrm{Ham}}_{\Delta t} = \Delta t^3 \xi_+ + \Delta t^4 r_{\Delta t}\,, \tag{13}$$

with $\sup_{0<\Delta t\leqslant\Delta t^*}\|r_{\Delta t}\|_{L^\infty_{\mathcal{K}_\alpha}} \leqslant K$. *Moreover, the leading order of the rejection rate is given by* $\xi_+ := \max(0,\xi)$ *with*

$$\xi = -\mathcal{L}_{\rm Ham} H_2, \qquad H_2(q,p) = \frac{1}{12}\left[-\frac{1}{2}\nabla V(q)^T\nabla^2 U(p)\nabla V(q) + \nabla U(p)^T\nabla^2 V(q)\nabla U(p)\right]. \tag{14}$$

As discussed in the introduction, the crucial part of the sampling usually is the sampling of the marginal of the canonical measure μ in the position variable. There is therefore some freedom in the choice of U. The expression of the rejection rate (14) suggests that U should be chosen such that derivatives of order up to 3 are not too large, in order for $\bar{\xi}$ to be as small as possible. This remark is used in Section 4 to improve the kinetic energy functions currently considered in adaptively restrained Langevin dynamics.

Proof. The idea of the proof is that, according to results of backward analysis [11], the first order modified Hamiltonian $H + \Delta t^2 H_2$ should be preserved at order Δt^5 over one timestep. The rejection rate is therefore given, at dominant order, by $-\Delta t^2[H_2(\Phi_{\Delta t}(q,p)) - H_2(q,p)] \simeq -\Delta t^3(\mathcal{L}_{\rm Ham}H_2)(q,p)$.

To identify H_2 and make the previous reasoning rigorous, we write the proposal (10) as

$$\Phi_{\Delta t}(q,p) = \begin{pmatrix} q + \nabla U\left(p - \nabla V(q)\dfrac{\Delta t}{2}\right)\Delta t, \\ p - \nabla V(q)\dfrac{\Delta t}{2} - \nabla V\left(q + \nabla U\left(p - \nabla V(q)\dfrac{\Delta t}{2}\right)\Delta t\right)\dfrac{\Delta t}{2}\end{pmatrix},$$

so that

$$\begin{aligned}\Phi_{\Delta t}(q,p) = \begin{pmatrix} q \\ p\end{pmatrix} + \Delta t\begin{pmatrix}\nabla U(p) \\ -\nabla V(q)\end{pmatrix} - \frac{\Delta t^2}{2}\begin{pmatrix}\nabla^2 U(p)\nabla V(q) \\ \nabla^2 V(q)\nabla U(p)\end{pmatrix} \\ + \frac{\Delta t^3}{4}\begin{pmatrix}\frac{1}{2}D^3U(p):\nabla V(q)^{\otimes 2} \\ \nabla^2 V(q)\nabla^2 U(p)\nabla V(q) - D^3V(q):\nabla U(p)^{\otimes 2}\end{pmatrix} + \Delta t^4 R_{\Delta t}(q,p),\end{aligned} \tag{15}$$

where the remainder $R_{\Delta t}(q,p)$ grows at most polynomially in (q,p), uniformly in Δt (this is easily seen by performing Taylor expansions with integral remainders). Denoting by $y = (q,p)^T$, we note that the Hamiltonian dynamics (9) can be reformulated as

$$\dot{y} = F(y), \qquad F(y) = \begin{pmatrix}\nabla U(p) \\ -\nabla V(q)\end{pmatrix}.$$

This implies that

$$\ddot{y} = DF(y)F(y) = -\begin{pmatrix}\nabla^2 U(p)\nabla V(q) \\ \nabla^2 V(q)\nabla U(p)\end{pmatrix},$$

and

$$\dddot{y} = \begin{pmatrix} D^3U(p):\nabla V(q)^{\otimes 2} - \nabla^2 U(p)\nabla^2 V(q)\nabla U(p) \\ -D^3V(p):\nabla U(p)^{\otimes 2} + \nabla^2 V(q)\nabla^2 U(p)\nabla V(q)\end{pmatrix}.$$

Therefore, denoting by ϕ_t the flow of the Hamiltonian dynamics (9), it holds

$$\Phi_{\Delta t}(q,p) = \phi_{\Delta t}(q,p) + \Delta t^3 G(q,p) + \Delta t^4 \widetilde{R}_{\Delta t}(q,p), \tag{16}$$

where

$$G(q,p) = \frac{1}{12}\begin{pmatrix} -\frac{1}{2}D^3U(p):\nabla V(q)^{\otimes 2} + 2\nabla^2 U(p)\nabla^2 V(q)\nabla U(p) \\ -D^3V(q):\nabla U(p)^{\otimes 2} + \nabla^2 V(q)\nabla^2 U(p)\nabla V(q)\end{pmatrix},$$

and the remainder $\widetilde{R}_{\Delta t}(q,p)$ grows at most polynomially in (q,p) uniformly in Δt. A simple computation shows that

$$G = \begin{pmatrix} \nabla_p H_2(q,p) \\ -\nabla_q H_2(q,p) \end{pmatrix},$$

with H_2 defined in (14). Note that for the standard kinetic energy U_{std}, this expression reduces to the one derived in [10, 25].

From the error estimate (16), we compute

$$\begin{aligned} H(\Phi_{\Delta t}(q,p)) - H(q,p) &= H(\phi_{\Delta t}(q,p)) - H(q,p) + \Delta t^3 G(q,p)\nabla H(q,p) + \Delta t^4 \widehat{R}_{\Delta t}(q,p) \\ &= -\Delta t^3 \mathcal{L}_{\mathrm{Ham}} H_2(q,p) + \Delta t^4 \widehat{R}_{\Delta t}(q,p), \end{aligned}$$

where the remainder $\widehat{R}_{\Delta t}(q,p)$ grows at most polynomially in (q,p) uniformly in Δt. This allows to identify $\xi = -\mathcal{L}_{\mathrm{Ham}} H_2$ as the leading order term of the energy variation over one step. In order to compute the expected rejection rate, we rely on the inequality

$$x_+ - \frac{x_+^2}{2} \leqslant 1 - \min\left(1, \mathrm{e}^{-x}\right) \leqslant x_+, \quad x_+ = \max(0,x).$$

This implies that

$$0 \leqslant A_{\Delta t}^{\mathrm{Ham}}\left(q^n, p^n\right) = \Delta t^3 \xi_+\left(q^n, p^n\right) + \Delta t^4 \mathscr{R}_{\Delta t}(q^n, p^n), \tag{17}$$

where the remainder $\mathscr{R}_{\Delta t}$ grows at most polynomially in (q,p) uniformly in Δt, which concludes the proof. □

As a corollary of the estimates (13) on the rejection rate and the consistency result (16) for the scheme without rejections, we can obtain weak-type expansions for the evolution operator

$$\begin{aligned} P_{\Delta t}^{\mathrm{Ham}}\varphi(q,p) &= \mathbb{E}_{\mathcal{U}}\left[\Psi_{\Delta t}^{\mathrm{Ham}}(q,p,\mathcal{U})\right] \\ &= \varphi\left(\Phi_{\Delta t}(q,p)\right) + \left(1 - A_{\Delta t}^{\mathrm{Ham}}(q,p)\right)\Big(\varphi(q,-p) - \varphi(\Phi_{\Delta t}(q,p))\Big). \end{aligned}$$

Since $A_{\Delta t}^{\mathrm{Ham}}(q,p) \in [0,1]$ and $\Phi_{\Delta t}(q,p)$ grows at most polynomially in (q,p) uniformly in Δt, a direct inspection of the latter expression shows that the operator $P_{\Delta t}^{\mathrm{Ham}}$ maps functions growing at most polynomially into functions growing at most polynomially: for any $\alpha \in \mathbb{N}$, there exist $\alpha' \in \mathbb{N}$ and $C_\alpha > 0$ such that

$$\forall f \in L^\infty_{\mathcal{K}_\alpha}, \qquad \left\|P_{\Delta t}^{\mathrm{Ham}} f\right\|_{L^\infty_{\mathcal{K}_\alpha}} \leqslant C_\alpha \|f\|_{L^\infty_{\mathcal{K}_{\alpha'}}}. \tag{18}$$

In order to understand the behavior of the evolution operator for small Δt, we first note that, for instance by the techniques reviewed in [16, Section 4.3], it can be shown that, for any $\varphi \in \mathscr{S}$,

$$\varphi\left(\Phi_{\Delta t}(q,p)\right) = \varphi + \Delta t \mathcal{L}_{\mathrm{Ham}}\varphi + \frac{\Delta t^2}{2}\mathcal{L}_{\mathrm{Ham}}^2\varphi + \Delta t^3 R_{\Delta t}^{\mathrm{Verlet}}\varphi,$$

where $R_{\Delta t}^{\mathrm{Verlet}}\varphi$ grows at most polynomially in (q,p) uniformly in Δt. Therefore, by (17),

$$P_{\Delta t}^{\mathrm{Ham}}\varphi = \varphi + \Delta t \mathcal{L}_{\mathrm{Ham}}\varphi + \frac{\Delta t^2}{2}\mathcal{L}_{\mathrm{Ham}}^2\varphi + \Delta t^3 R_{\Delta t}^{\mathrm{Ham}}\varphi, \tag{19}$$

where the remainder

$$R_{\Delta t}^{\mathrm{Ham}}\varphi(q,p) = \left(1 - A_{\Delta t}^{\mathrm{Ham}}(q,p)\right)\Big(\varphi(q,-p) - \varphi(\Phi_{\Delta t}(q,p))\Big) + R_{\Delta t}^{\mathrm{Verlet}}\varphi(q,p).$$

grows at most polynomially in (q,p) uniformly in Δt.

3.2 Discretization of the fluctuation/dissipation

In order to construct a GHMC scheme for (1), we need to generate momenta distributed according to

$$\kappa(dp) = Z_\kappa^{-1} \mathrm{e}^{-\beta U(p)}\, dp, \tag{20}$$

which are then used as initial conditions in the Hamiltonian part of the scheme. This can be achieved through a discretization of the fluctuation-dissipation, corrected by a Metropolis procedure.

We use here a scheme proposed in [9] for the elementary dynamics (6). The proposal function is given by

$$\widetilde{p}^{n+1} = \Phi_{\Delta t}^{\mathrm{FD}}(p^n, G^n) = p^n - \gamma \nabla U \left(p^n + \frac{1}{2}\sqrt{\frac{2\gamma\Delta t}{\beta}} G^n \right) \Delta t + \sqrt{\frac{2\gamma\Delta t}{\beta}} G^n \,, \tag{21}$$

where $(G^n)_{n\geqslant 0}$ is a sequence of i.i.d. standard d-dimensional Gaussian random variables. It seems that the computation of the probability density of going from a given momentum p to a new one p' is difficult since $\Phi_{\Delta t}^{\mathrm{FD}}(p, G)$ depends nonlinearly on G. It turns out however that the proposal (21) can itself be interpreted as the output of some one-step HMC scheme, starting from a random conjugate variable $R^n := G^n/\sqrt{\beta} \in \mathbb{R}^d$ and for an effective timestep $h = \sqrt{2\gamma\Delta t}$:

$$\left\{ \begin{array}{l} p^{n+1/2} = p^n + R^n \dfrac{h}{2}, \\ R^{n+1} = R^n - \nabla U(p^{n+1/2}) h, \\ \widetilde{p}^{n+1} = p^{n+1/2} + R^{n+1} \dfrac{h}{2}. \end{array} \right. \tag{22}$$

The Hamiltonian dynamics which is discretized by this scheme is the one associated with the energy

$$E(p, R) = U(p) + \frac{1}{2} R^2.$$

Therefore, the acceptance rule for the proposal (21) is

$$A_{\Delta t}^{\mathrm{FD}}(p^n, G^n) = \min\left(1, \exp\left(-\beta \Big[E\left(\widetilde{p}^{n+1}, R^{n+1}\right) - E(p^n, R^n) \Big]\right)\right).$$

In summary, the new momentum is therefore given by

$$p^{n+1} = \Psi_{\Delta t}^{\mathrm{FD}}(p^n, G^n, \mathcal{U}^n) = p^n + \mathbb{1}_{\left\{\mathcal{U}^n \leqslant A_{\Delta t}^{\mathrm{FD}}(p^n, G^n)\right\}} \left(\Phi_{\Delta t}^{\mathrm{FD}}(p^n, G^n) - p^n \right). \tag{23}$$

Remark 3.2. Note that the efficiency of the Metropolization procedure of the fluctuation/dissipation does not degrade as the dimension increases in the case when the kinetic energy is a sum of individual contributions:

$$U(p) = \sum_{i=1}^{d} u(p_i).$$

In this case, the dynamics in each component can indeed be Metropolized independently of the other components.

In [9], the properties of the scheme (21) were studied for compact spaces. It is however possible to adapt some of the results obtained in this work when $U(p)$ and all its derivatives grow at most polynomially, and the marginal κ defined in (20) admits moments of all orders. In this case, the rejection rate scales as $\Delta t^{3/2}$ (which in fact can also be obtained directly from

Lemma 3.1 for the effective timestep $h = \sqrt{2\gamma\Delta t}$). Moreover, since $\Phi^{\rm FD}_{\Delta t}(p,G)$ grows at most polynomially in (p,G) uniformly in Δt, the evolution operator

$$\begin{aligned} P^{\rm FD}_{\Delta t}\varphi(p) &= \mathbb{E}_{\mathcal{U},G}\left[\varphi\left(\Psi^{\rm FD}_{\Delta t}(p,G,\mathcal{U})\right)\right] \\ &= \mathbb{E}_G\left[A^{\rm FD}_{\Delta t}(p,G)\varphi\left(\Phi^{\rm FD}_{\Delta t}(p,G)\right)\right] + \left(1-\mathbb{E}_G\left[A^{\rm FD}_{\Delta t}(p,G)\right]\right)\varphi(p), \end{aligned}$$

maps functions growing at most polynomially into functions growing at most polynomially: for any $\alpha \in \mathbb{N}$, there exist $\alpha' \in \mathbb{N}$ and $C_\alpha > 0$ such that

$$\forall f \in L^\infty_{\mathcal{K}_\alpha}, \qquad \left\|P^{\rm FD}_{\Delta t} f\right\|_{L^\infty_{\mathcal{K}_\alpha}} \leqslant C_\alpha \|f\|_{L^\infty_{\mathcal{K}_{\alpha'}}}. \tag{24}$$

Finally, the following weak-type expansion holds true by [9, Lemma 3]: for $\varphi \in \mathscr{S}$,

$$P^{\rm FD}_{\Delta t}\varphi = \varphi + \Delta t \mathcal{L}_{\rm FD}\varphi + \frac{\Delta t^2}{2}\mathcal{L}^2_{\rm FD}\varphi + \Delta t^{5/2} R^{\rm FD}_{\Delta t}\varphi, \tag{25}$$

where the remainder $R^{\rm FD}_{\Delta t}\varphi$ grows at most polynomially in (q,p) uniformly in Δt.

3.3 Complete Generalized Hybrid Monte-Carlo scheme

The complete scheme for the metropolized Langevin dynamics with general kinetic energy is obtained by concatenating the updates (12) and (23). Depending on whether Lie or Strang splittings are considered, and also on the order in which the operations are performed, several schemes can be considered. For instance, the scheme characterized by the evolution operator $P^{\rm GHMC}_{\Delta t} = P^{\rm FD}_{\Delta t} P^{\rm Ham}_{\Delta t}$ corresponds to first updating the momenta with (23), and then updating both positions and momenta according to (12).

All such splitting schemes preserve the invariant measure μ by construction. They are also all of weak order at least 1. A second weak order accuracy can however be obtained for Strang splittings, as made precise in the following lemma.

Lemma 3.3. *Consider $P^{\rm GHMC}_{\Delta t} = P^{\rm FD}_{\Delta t/2} P^{\rm Ham}_{\Delta t} P^{\rm FD}_{\Delta t/2}$ or $P^{\rm GHMC}_{\Delta t} = P^{\rm Ham}_{\Delta t/2} P^{\rm FD}_{\Delta t} P^{\rm Ham}_{\Delta t/2}$. Then, for any $\varphi \in \mathscr{S}$, there exist $\Delta t^*, K, \alpha > 0$ such that*

$$P^{\rm GHMC}_{\Delta t}\varphi = \varphi + \Delta t \mathcal{L}\varphi + \frac{\Delta t^2}{2}\mathcal{L}^2\varphi + \Delta t^{5/2} r_{\Delta t,\varphi}, \tag{26}$$

where $\sup_{0<\Delta t\leqslant\Delta t^*} \|r_{\Delta t,\varphi}\|_{L^\infty_{\mathcal{K}_\alpha}} \leqslant K$.

Proof. This result is a direct consequence of the estimates (19)-(25). We however sketch the proof for completeness. Fix $\varphi \in \mathscr{S}$. In view of (25),

$$P^{\rm FD}_{\Delta t/2} P^{\rm Ham}_{\Delta t} P^{\rm FD}_{\Delta t/2}\varphi = P^{\rm FD}_{\Delta t/2} P^{\rm Ham}_{\Delta t}\widetilde{\varphi} + \Delta t^{5/2} P^{\rm FD}_{\Delta t/2} P^{\rm Ham}_{\Delta t} R^{\rm FD}_{\Delta t}\varphi,$$

where

$$\widetilde{\varphi} = \left(\mathrm{Id} + \frac{\Delta t}{2}\mathcal{L}_{\rm FD} + \frac{\Delta t^2}{8}\mathcal{L}^2_{\rm FD}\right)\varphi \in \mathscr{S}.$$

The remainder $P^{\rm FD}_{\Delta t/2} P^{\rm Ham}_{\Delta t} R^{\rm FD}_{\Delta t}\varphi$ grows at most polynomially in (q,p) uniformly in Δt by (18)-(24). We next use (19) to write

$$P^{\rm FD}_{\Delta t/2} P^{\rm Ham}_{\Delta t}\widetilde{\varphi} = P^{\rm FD}_{\Delta t/2}\widehat{\varphi} + \Delta t^3 P^{\rm FD}_{\Delta t/2} R^{\rm Ham}_{\Delta t}\widetilde{\varphi},$$

where

$$\widehat{\varphi} = \left(\mathrm{Id} + \Delta t\mathcal{L}_{\rm Ham} + \frac{\Delta t^2}{2}\mathcal{L}^2_{\rm Ham}\right)\left(\mathrm{Id} + \frac{\Delta t}{2}\mathcal{L}_{\rm FD} + \frac{\Delta t^2}{8}\mathcal{L}^2_{\rm FD}\right)\varphi \in \mathscr{S}.$$

The remainder $P^{\rm FD}_{\Delta t/2} R^{\rm Ham}_{\Delta t} \widetilde{\varphi}$ grows at most polynomially in (q,p) uniformly in Δt by (24). By applying again (25), we finally obtain that

$$P^{\rm FD}_{\Delta t/2} P^{\rm Ham}_{\Delta t} P^{\rm FD}_{\Delta t/2} \varphi = \Delta t^{5/2} \mathcal{R}_{\Delta t, \varphi} + \left({\rm Id} + \frac{\Delta t}{2} \mathcal{L}_{\rm FD} + \frac{\Delta t^2}{8} \mathcal{L}^2_{\rm FD} \right) \left({\rm Id} + \Delta t \mathcal{L}_{\rm Ham} + \frac{\Delta t^2}{2} \mathcal{L}^2_{\rm Ham} \right) \left({\rm Id} + \frac{\Delta t}{2} \mathcal{L}_{\rm FD} + \frac{\Delta t^2}{8} \mathcal{L}^2_{\rm FD} \right) \varphi,$$

where the remainder $\mathcal{R}_{\Delta t, \varphi}$ grows at most polynomially in (q,p) uniformly in Δt. The conclusion follows by expanding the last term on the right-hand side, grouping together terms of order Δt and Δt^2, and gathering the higher order terms in the remainder. □

As corollary of the weak error expansion (26), error estimates on dynamical properties such as integrated correlation functions can be deduced with the techniques from [16] provided an exponential convergence of $(P^{\rm GHMC}_{\Delta t})^n \varphi$ towards $\mathbb{E}_\mu(\varphi)$ is proved in the spaces $L^\infty_{\mathcal{K}_\alpha}$, with a rate depending on the physical time $n\Delta t$, uniformly in Δt. A typical way to obtain such estimates is to establish a Lyapunov condition for the functions $\mathcal{K}_\alpha$ and a minorization condition on a compact space, in order to apply the results from [21, 12]. Although we were able to prove a minorization condition in the case when $U - U_{\rm std}$ is bounded and the position space $\mathcal{D}$ is compact (see [26]), we were not able to establish a Lyapunov condition. The problem is that, even for compact position spaces and standard, quadratic kinetic energies, the rejection rate of the fluctuation/dissipation part of the scheme degenerates as $|p| \to +\infty$. Such difficulties were already encountered in the study of Metropolized Langevin-type algorithms on unbounded spaces, where the problem was taken care of by an appropriate truncation of the accessible space [5].

4 Adaptively restrained Langevin dynamics

The Adaptively Restrained Particle Simulation method was proposed in [2] in order to reduce the computational complexity of the forces update. The aim of this section is to devise better kinetic energy functions for the adaptively restrained (AR) Langevin dynamics, allowing for larger timesteps in the simulations. We start by recalling the kinetic energy function used in the original AR Langevin dynamics [2] in Section 4.1, where we also propose an alternative kinetic energy function. The relevance of this alternative energy function is studied in Section 4.2, where we use the rejection rates of the GHMC algorithm to quantify the stability of the schemes under consideration. In essence, we fix an admissible rejection rate, and find the largest timestep for which the rejection is lower or equal to this tolerance.

4.1 Kinetic energy functions for AR Langevin

In AR Langevin, the standard kinetic energy is replaced by a kinetic energy which vanishes for small values of momenta and matches the standard kinetic energy for sufficiently large values of momenta. The transition between these two regions is made in the original model [2] by an interpolation spline $s_{\rm org}$ which ensures the regularity of the transition on the kinetic energy itself. More precisely, introducing two energy parameters $0 < e_{\rm min} < e_{\rm max}$,

$$U_{\rm org}(p) = \sum_{i=1}^N u(p_i) \quad \text{where} \quad u(p_i) = \begin{cases} 0 & \text{for} \quad \dfrac{p_i^2}{2m_i} \leqslant e_{\rm min}, \\ s_{\rm org}\left(\dfrac{p_i^2}{2m_i} \right) & \text{for} \quad \dfrac{p_i^2}{2m_i} \in [e_{\rm min}, e_{\rm max}], \\ \dfrac{p_i^2}{2m_i} & \text{for} \quad \dfrac{p_i^2}{2m_i} \geqslant e_{\rm max}. \end{cases} \tag{27}$$

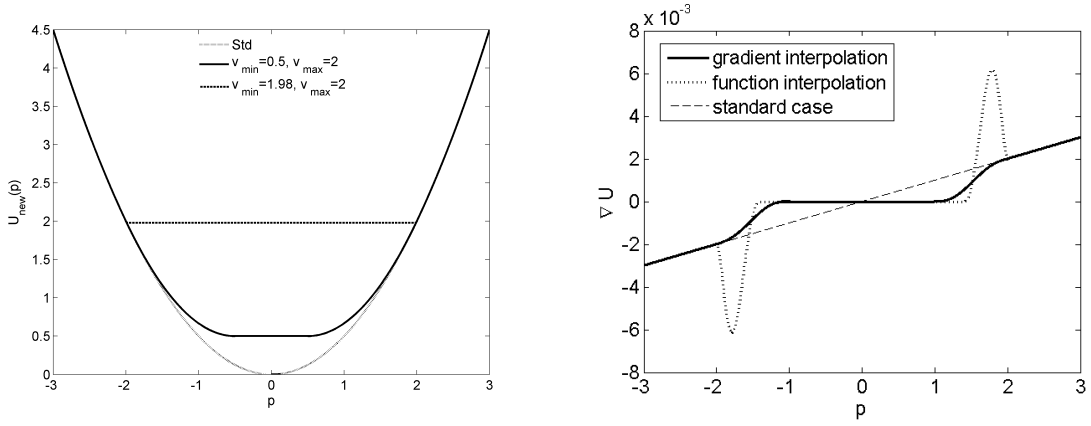

(a) The AR-kinetic energy function (28) for various choice of parameters $v_{\min}$ and $v_{\max}$.

(b) Gradient interpolation of the kinetic energy (U_{new}) versus function interpolation (U_{org}).

Figure 1: Comparison between the AR-kinetic energy function (28) and the original AR kinetic energy (27).

The function s_{org} is such that $x \mapsto s_{\text{org}}(x)\,\mathbb{1}_{x\in[e_{\min},e_{\max}]} + x\,\mathbb{1}_{x>e_{\max}}$ is C^2. The original AR Langevin kinetic energy was motivated by some physical interpretation in terms of momentum-dependent masses. One unpleasant feature of the definition (27) is that the derivatives ∇U which appear in the dynamics (1) are typically large at the transition points (see Figure 1b). Since the dynamics is determined by ∇U, a more satisfactory approach seems to interpolate the kinetic force ∇U between 0 in the region of small momenta and $M^{-1}p$ in the region of large momenta. We introduce to this end a second spline function s_{new} and define, for two velocity parameters $0 < v_{\min} < v_{\max}$,

$$U_{\text{new}}(p) = \sum_{i=1}^{d} u(p_i) \quad \text{where} \quad u(p_i) = \begin{cases} S_{v_{\min}v_{\max}} \text{ for } \dfrac{|p_i|}{m_i} \leqslant v_{\min}, \\ s_{\text{new}}\left(p_i\right) \text{ for } \dfrac{|p_i|}{m_i} \in [v_{\min}, v_{\max}], \\ \dfrac{p_i^2}{2m_i} \text{ for } \dfrac{|p_i|}{m_i} \geqslant v_{\max} \end{cases} \tag{28}$$

where $S_{v_{\min}v_{\max}}$ is a constant ensuring the continuity of the kinetic energy. Figure 1a represents the alternative kinetic energy (28) as a function of the momenta for various choices of the parameters. Figure 1b compares the derivatives of the original and new kinetic energies. Note that the alternative kinetic energy (28) leads to a smaller maximal value of the kinetic force ∇U than the original AR kinetic energy (27). This is also true for higher order derivatives of U.

It is difficult to directly compare the canonical distributions of momenta associated with U_{org} and U_{new}. For instance, it is not possible in general to ensure that these two distributions coincide for small and large momenta, because of the normalization constant in the probability distribution. In the sequel, we consider $e_{\min} = m_i v_{\min}^2/2$ and $e_{\max} = m_i v_{\max}^2/2$ for the ith particle, in order to have a constant kinetic energy (resp. a standard kinetic energy) in the same energy intervals.

4.2 Determining the best kinetic energy function

Since the AR-kinetic energy in general has derivatives larger than the ones of the standard kinetic energy, the timestep should be reduced in order to preserve the stability of the numerical method.

We characterize in this section the possible reduction of the timestep due to the modification of the kinetic energy. As described in Section 3.3, we metropolize the AR-Langevin dynamics by first integrating the Hamiltonian with (12) and then the fluctuation-dissipation part with (23). This corresponds to the evolution operator $P_{\Delta t}^{\mathrm{GHMC}} = P_{\Delta t}^{\mathrm{Ham}} P_{\Delta t}^{\mathrm{FD}}$.

Recall that the average rejection rate of the Hamiltonian and fluctuation/dissipation parts, namely (with expectations over $(q,p) \sim \mu$ and over the random variables G,$\mathcal{U}$ used in the updates)

$$\mathcal{R}^{\mathrm{Ham}}(\Delta t) := \mathbb{E}\left(1 - A_{\Delta t}^{\mathrm{Ham}}\right), \qquad \mathcal{R}^{\mathrm{FD}}(\Delta t) := \mathbb{E}\left[1 - A_{\Delta t}^{\mathrm{FD}}(\Psi(p, G, \mathcal{U}))\right],$$

respectively scale as Δt^3 and $\Delta t^{3/2}$ (see Lemma 3.1). We consider three kinds of AR-kinetic energies: the original function interpolation (27), and two interpolation functions (28) based on the gradient. More precisely, we either choose a linear spline or a C^2 spline by a polynomial of order 5 on the gradient ∇U. The corresponding kinetic energies are respectively C^2 and C^3. The aim is to check the scaling of the rejection rates in terms of powers of Δt, and to estimates the prefactors for the various kinetic energies.

We consider a system of 64 particles of mass $m_i = 1$ in a three dimensional periodic box with particle density $\rho = 0.56$. The particles interact by a purely repulsive WCA pair potential, which is a truncated Lennard-Jones potential [24]:

$$V_{\mathrm{WCA}}(r) = \begin{cases} 4\varepsilon_{\mathrm{LJ}}\left[\left(\frac{\sigma_{\mathrm{LJ}}}{r}\right)^{12} - \left(\frac{\sigma_{\mathrm{LJ}}}{r}\right)^{6}\right] + \varepsilon_{\mathrm{LJ}} & \text{if } r \leqslant r_0, \\ 0 & \text{if } r > r_0, \end{cases}$$

where r denotes the distance between two particles, $\varepsilon_{\mathrm{LJ}}$ and σ_{LJ} are two positive parameters and $r_0 = 2^{1/6}\sigma_{\mathrm{LJ}}$. In our simulations the parameters of the potential are set to $\varepsilon_{\mathrm{LJ}} = 1, \sigma_{\mathrm{LJ}} = 1$, while the parameters of the AR-Langevin dynamics (1) are set to $\gamma = 1, \beta = 1$.

Figure 2 shows the average rejection rates for the AR parameters $v_{\max} = 2$ and $v_{\min} = 1$ for U_{new}, as well as $e_{\max} = 2$ and $e_{\min} = 0.5$ for U_{org}. This choice of parameters corresponds to $\sim 30\%$ percent of particles which are frozen for both AR-kinetic energies, *i.e.* which are in the region where ∇U vanishes (see [27] for a thorough discussion on the link between the percentage of frozen particles and the algorithmic speed-up). Note that the predicted scalings of the rejection rates are recovered in all cases. The prefactor is however larger for the kinetic energy U_{org} from [2] than for U_{new}, especially for the fluctuation-dissipation part. The prefactor is also slightly smaller for the kinetic energy based on the gradient interpolation with a linear function, which is fortunate since ∇U has a lower computational cost than for interpolations based on higher order splines.

In order to quantify the dependence of the prefactors in the rejection rate on the concrete choice of the parameters in the kinetic energy function, we compute the relative deviation of the prefactor from the reference provided by simulations with the standard kinetic energy. Figure 3 plots for various values of the parameter $v_{\min}$ (for fixed $v_{\max} = 2$) the relative deviation between the prefactors inferred from simulation results such as the ones presented in Figure 2. To this end, we perform a least-square fit in a log-log scale to determine the prefactor C such that the rejection rate is approximately equal to $C\Delta t^{\alpha}$ (with $\alpha = 3$ for the Hamiltonian part, and $\alpha = 3/2$ for the fluctuation/dissipation). For each value of the parameters, we compute the relative variation of the prefactor with respect to the reference prefactor C_{std} provided by the rejection rate obtained for the standard kinetic energy:

$$\delta C = \frac{C}{C_{\mathrm{std}}} - 1.$$

The relative variation δC depends on the parameters $v_{\min}, v_{\max}$ (or $e_{\min}, e_{\max}$, depending on the context). As $v_{\min} \to v_{\max}$, the derivatives of the kinetic energy function have larger absolute

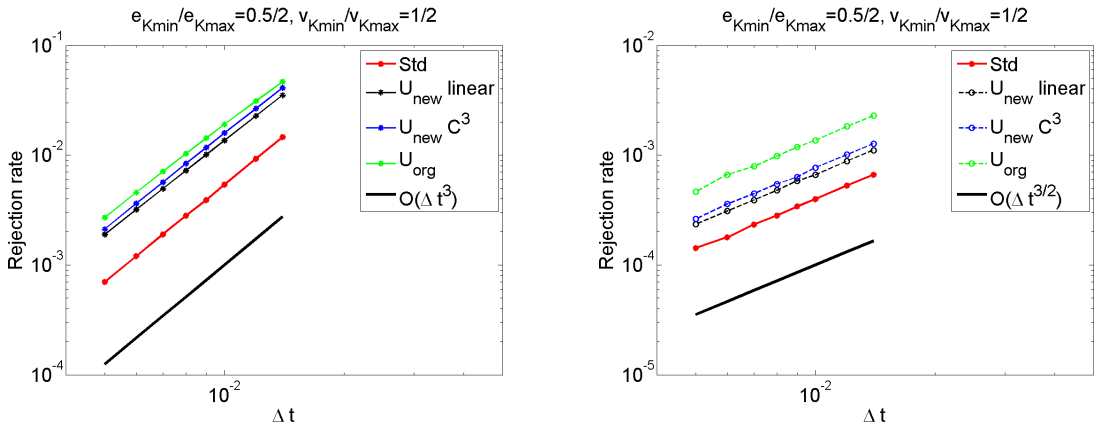

(a) Hamiltonian part

(b) Fluctuation-dissipation part.

Figure 2: Average rejection rates of GHMC as a function of the timestep for various kinetic energies (see text). The scaling of the rejection rates corresponds to the predicted orders, *i.e.* Δt^3 for the Hamiltonian part and $\Delta t^{3/2}$ for the fluctuation-dissipation part.

values (recall Figure 1b). The dynamics is therefore less stable, which translates into larger values of the prefactor in the rejection rate as $v_{\min}$ increases (see Figure 3). Moreover, the relative increase of the prefactor is larger for $U_{\rm org}$ than for $U_{\rm new}$. In conclusion, the new definition of the AR-kinetic energy improves the numerical properties of the method, as demonstrated by a smaller prefactor in the rejection rate of the GHMC scheme.

We are now in position to determine the variations in the admissible timesteps as a function of the kinetic energies. We fix to this end a rejection rate, for the Hamiltonian part since this subdynamics mixes information on the positions and momenta, and involves the forces $-\nabla V(q)$ which are often at the origin of the stability limitations. Similar results are however obtained for the fluctuation/dissipation part, see [26].

In our tests, we set the target rejection rate to two values: $\mathcal{R}^{\rm Ham}(\Delta t) = 0.001$ and $\mathcal{R}^{\rm Ham}(\Delta t) = 0.5$. Figure 4 presents the timesteps Δt achieving the desired rejection rates (normalized by $\Delta t_{\rm std}$, the timestep corresponding to the given rejection rate for the standard quadratic energy), for the kinetic energy $U_{\rm new}$ (with an interpolation spline such that $U_{\rm new} \in C^3$) and for various values of the parameters. We observe that the timestep should be reduced with respect to the standard case when the transition becomes somewhat sharper, *i.e.* for δ approaching 1. Surprisingly, we observe that for smaller values of δ, the timestep can in fact be increased compared to standard Langevin dynamics.

5 Decreasing metastability with modified kinetic energies

We finally illustrate an alternative use of the modified kinetic energy function. We demonstrate by a simple example that the modification of the dynamics can lead to a faster exploration of the phase-space. An exploration of this idea for high dimensional problems requires further work (in progress [26]).

We study two dimensional systems (*i.e* $q = (x, y) \in \mathbb{R}^2$) for the potential similar to the one considered in [17, Section 1.3.3.1]:

$$V(x,y) = \frac{1}{6}\left(4\left(-x^2-y^2+w\right)^2 + 10\left(x^2-2\right)^2 + \left((x+y)^2-1\right)^2 + \left((x-y)^2-1\right)^2\right). \quad (29)$$

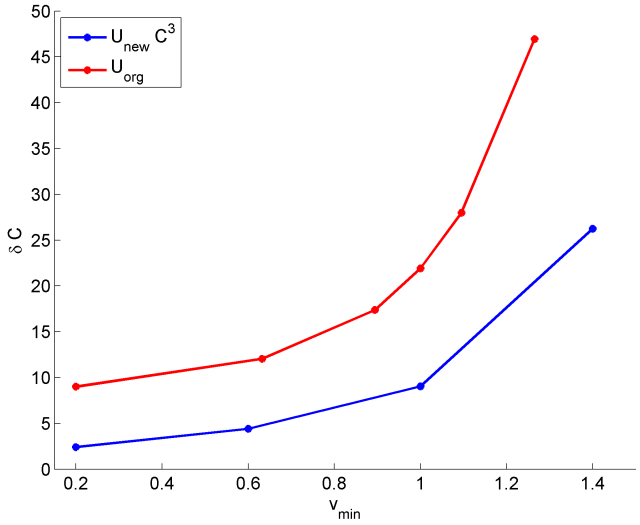

Figure 3: Relative deviation of the prefactor in the scaling of the average rejection for the Hamiltonian part as a function of the timestep Δt. The data is extracted from the results presented in Figure 2a.

This potential can be seen as some effective double well potential in the x direction (see Figure 5 for contour plots). The metastability of Langevin dynamics is caused by some energetic barrier in this direction at $x = 0$. In the following numerical experiments, we discretize the Langevin dynamics (1) by the same scheme as in Section 4, with $\gamma = 1$, $m = 1$ and $\Delta t = 0.001$.

Various kinetic energies can be considered. We focus on the following ones:

(1) the standard kinetic energy $U_1(x, y) = (x^2 + y^2)/2$;

(2) a fifth order polynomial in both directions $U_2(x, y) = \left(|x|^5 + |y|^5\right)/5$, which provides an example of light-tailed distribution of momenta;

(3) a heavy tailed function distribution of momenta, corresponding to the choice

$$U_3(x, y) = \frac{4}{5}\left[|x|^{5/4} + |y|^{5/4}\right];$$

(4) the same function as the potential function $U_4 \equiv V$;

(5) a double-well function in the x-direction and a quadratic function in the $y-$direction:

$$U_5(x, y) = V_{\mathrm{DW}}(x) + \frac{y^2}{2}, \qquad V_{\mathrm{DW}}(x) = \left(|x - 1|^{-2} + |x + 1|^{-2}\right)^{-1}.$$

This function somewhat approximates V, so we expect the distribution of momenta under the canonical measure associated with U_5 to be close to the one associated with U_4.

Figure 6 presents two realizations of the Langevin dynamics (1) for a physical time $T = 1000$ and an inverse temperature $\beta = 1$, for the choices U_1 and U_4 above. Note that, for the standard kinetic energy U_1, there is only one crossing from one well to the other during the simulation time. On the other hand, there are many more crossings for U_4.

In order to quantify the reduction of the metastability gained by modifying the kinetic energy function, we numerically estimate the expected hitting time between two sets separated by the

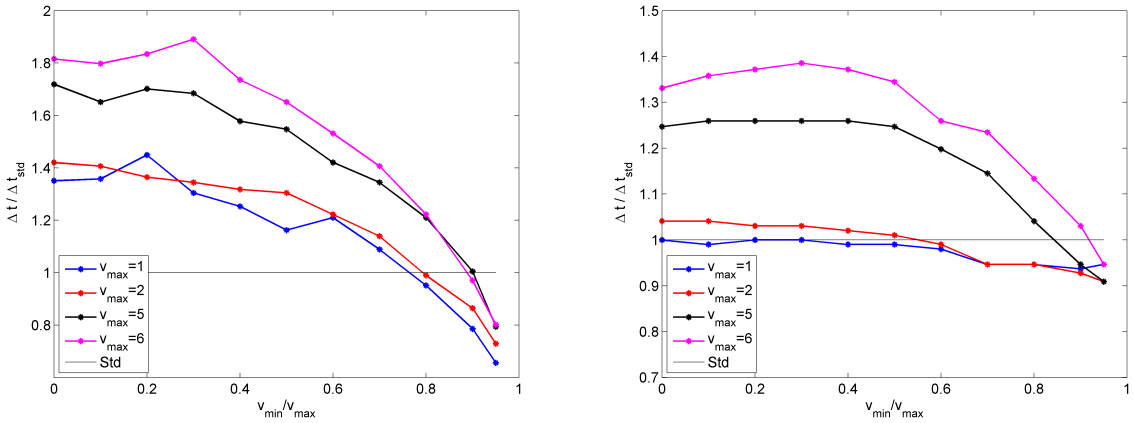

(a) Rejection rate fixed at 0.001

(b) Rejection rate fixed at 0.5

Figure 4: Timesteps normalized by Δt_{std} (the time step corresponding to the same rejection rate for the standard kinetic energy) corresponding to a fixed rejection rate in the Hamiltonian part for various values of $\delta = v_{\min}/v_{\max}$ and the kinetic energy (28).

energetic barrier. We start in fact from a given initial condition, which corresponds to the initial set $A := \{(1,0)\}$. We then compute the number of simulation steps necessary to reach the set $B := \{(x,y) : x \leqslant -1 \text{ and } |y| \leqslant 0.5\}$ (see Figure 5 for an illustration). The expected hitting time is estimated by an average over 1000 independent realizations of the exit process. We report in Table 1 the average physical time needed to reach the set B for each choice of the kinetic energy function, as well as the speed-up relative to the results obtained with the standard kinetic energy. Note that the hitting time is almost three time smaller with U_4. Intuitively, heavy tailed distributions of momenta (corresponding to U_3 here) could be thought

Kinetic energy	$U_1 = U_{\text{std}}$	U_2	U_3	U_4	U_5
T_{hit}	297.2 [±9.5]	259.2 [±7.8]	307.0 [±9.6]	101.7 [±3.2]	203.4 [±6.3]
Speed up $T_{\text{hit}}/T_{\text{std}}$	1	1.155	0.97	2.92	1.46

Table 1: Expected hitting times according to the choice of the kinetic energy functions U_i (see text). Errors bars determined by 95% confidence intervals are reported in brackets.

of as being interesting since they allow for larger velocities, which may facilitate the transition from one well to the other. This is however not the case. On the other hand, we observe that the double-well-like functions (U_4 and U_5) are most helpful to reduce the metastability of the dynamics and allow for more transitions from the region around $x = -1$ to the region around $x = 1$. Note that the hitting time is almost three time smaller with U_4. Moreover, in Figure 7, we plot the average physical time needed to reach the set B as a function of the inverse temperature β. We observe an exponential growth of the hitting time with respect to β which is characteristic for metastability caused by energetic barriers in the low temperature limit by the Eyring-Kramers law (see for instance the presentation and the references in [4, 18]). We fit the hitting times as

$$T_{\text{hit}}(\beta) = C\mathrm{e}^{\beta E},$$

for some energy level E. For the results presented in Figure 7, the energy level E is the same for all kinetic energies, but the prefactor C is different; in fact smaller for the modified kinetic

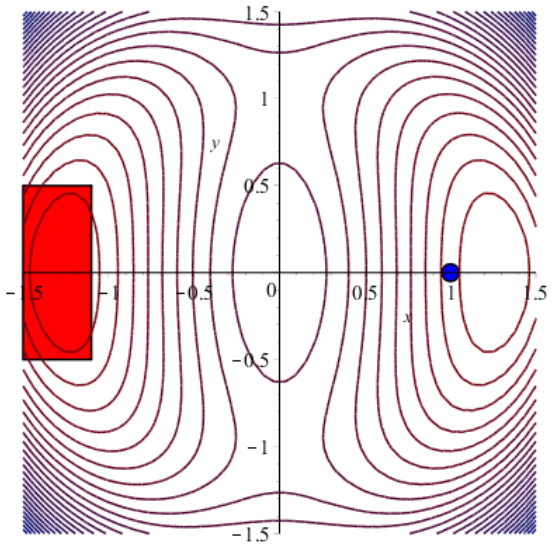

Figure 5: Two dimensional double-well potential (29). To compute exit times out of metastable states, we consider the starting configuration $A := (1, 0)$ and the target set $B := \{(x, y) : x \leqslant -1 \text{ and } |y| \leqslant 0.5\}$.

energy U_5 than for the standard kinetic energy U_1.

The excellent reduction in metastability we obtain on this simple low-dimensional system motivates us to test the relevance of this approch for higher dimensional systems. One track is to modify the kinetic energy on the velocity of some reaction coordinate summarizing slow degrees of freedom, keeping the standard kinetic energy for faster degrees of freedom; see [26] for preliminary steps in this direction.

Acknowledgments

This work was funded by the Agence Nationale de la Recherche, under grant ANR-14-CE23-0012 (COSMOS). Gabriel Stoltz benefited from the scientific environment of the Laboratoire International Associé between the Centre National de la Recherche Scientifique and the University of Illinois at Urbana-Champaign. Zofia Trstanova gratefully acknowledges funding from the European Research Council through the ERC StartingGrant No. 307629. We would like to thank to Sam Livingstone and Nawaf Bou-Rabee for fruitful discussions.

References

[1] A. Abdulle, G. Vilmart, and K. C. Zygalakis. Long time accuracy of Lie–Trotter splitting methods for Langevin dynamics. *SIAM Journal on Numerical Analysis*, 53(1):1–16, 2015.

[2] S. Artemova and S. Redon. Adaptively restrained particle simulations. *Phys. Rev. Lett.*, 109(19):190201, 2012.

[3] R. Balian. *From Microphysics to Macrophysics. Methods and Applications of Statistical Physics*, volume I - II. Springer, 2007.

[4] N. Berglund. Kramers' law: Validity, derivations and generalisations. *Markov Processes Relat. Fields*, 19:459–490, 2013.

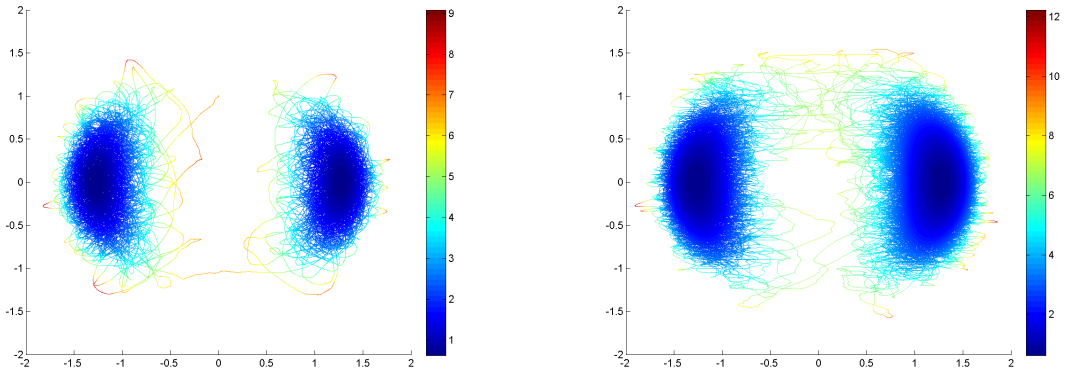

(a) Standard kinetic energy function.

(b) Same kinetic energy function as the potential energy function, *i.e.* $U \equiv V$.

Figure 6: Positions as a function of time for the modified Langevin dynamics with the two-dimensional double well potential (29), and two different kinetic energy functions. The simulation time is $T = 1000$, and the same realization of the Brownian motion is used in both cases. For the same number of simulation steps, there are more crossings between the wells for the dynamics with the modified kinetic energy (Right) than for the standard one (Left). The coloring corresponds to the values of the potential energy.

[5] N. Bou-Rabee and M. Hairer. Nonasymptotic mixing of the MALA algorithm. *IMA J. Numer. Anal.*, 33:80–110, 2013.

[6] N. Bou-Rabee and H. Owhadi. Long-run accuracy of variational integrators in the stochastic context. *SIAM J. Numer. Anal.*, 48(1):278–297, 2010.

[7] N. Bou-Rabee and E. Vanden-Eijnden. Pathwise accuracy and ergodicity of metropolized integrators for SDEs. *Commun. Pure Appl. Math.*, 63(5):655–696, 2009.

[8] S. Duane, A. D. Kennedy, B. J. Pendleton, and D. Roweth. Hybrid Monte Carlo. *Phys. Lett. B*, 195(2):216–222, 1987.

[9] M. Fathi and G. Stoltz. Improving dynamical properties of stabilized discretizations of overdamped Langevin dynamics. *arXiv preprint*, 1505.04905, 2015.

[10] E. Hairer, C. Lubich, and G. Wanner. Geometric numerical integration illustrated by the Störmer–Verlet method. *Acta numerica*, 12:399–450, 2003.

[11] E. Hairer, C. Lubich, and G. Wanner. *Geometric Numerical Integration: Structure-Preserving Algorithms for Ordinary Differential Equations*, volume 31. Springer, 2006.

[12] M. Hairer and J.C. Mattingly. Yet another look at Harris' ergodic theorem for Markov chains. In *Seminar on Stochastic Analysis, Random Fields and Applications VI*, volume 63 of *Progr. Probab.*, pages 109–117. Birkhäuser/Springer, 2011.

[13] W. K. Hastings. Monte Carlo sampling methods using Markov chains and their applications. *Biometrika*, 57:97–109, 1970.

[14] M. Kopec. Weak backward error analysis for Langevin process. *BIT*, 55:1057–1103, 2015.

[15] B. Leimkuhler and C. Matthews. *Molecular Dynamics: with deterministic and stochastic numerical methods*. Springer, 2015.

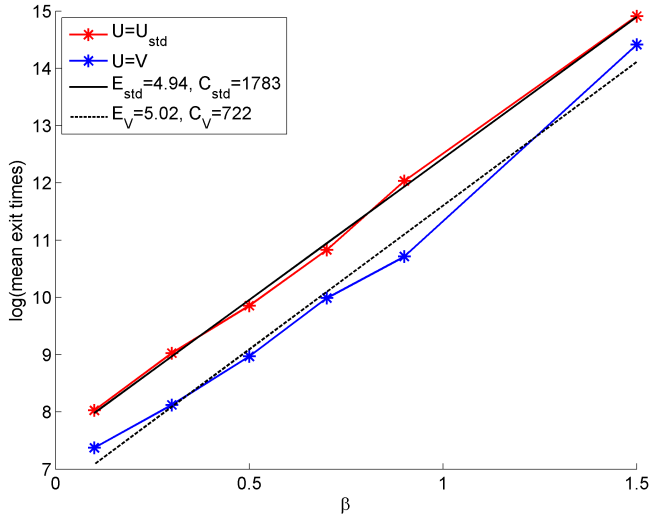

Figure 7: Mean exit times over 100 realizations as a function of $\beta \in \{0.1, 0.3, 0.5, 0.7, 0.9, 1.5\}$.

[16] B. Leimkuhler, Ch. Matthews, and G. Stoltz. The computation of averages from equilibrium and nonequilibrium Langevin molecular dynamics. *IMA J. Numer. Anal.*, 36(1):13–79, 2016.

[17] T. Lelièvre, M. Rousset, and G. Stoltz. *Free Energy Computations: A Mathematical Perspective*. Imperical College Press, 2010.

[18] T. Lelièvre and G. Stoltz. Partial differential equations and stochastic methods in molecular dynamics. *Acta Numerica*, 25:681–880, 2016.

[19] J. C Mattingly, A.M. Stuart, and D.J. Higham. Ergodicity for SDEs and approximations: locally Lipschitz vector fields and degenerate noise. *Stoch. Proc. Appl.*, 101(2):185–232, 2002.

[20] N. Metropolis, A. W. Rosenbluth, M. N. Rosenbluth, A. H. Teller, and E. Teller. Equations of state calculations by fast computing machines. *J. Chem. Phys.*, 21(6):1087–1091, 1953.

[21] S. P. Meyn and R. L. Tweedie. *Markov Chains and Stochastic Stability*. Springer, 2012.

[22] S. Redon, G. Stoltz, and Z. Trstanova. Error analysis of modified Langevin dynamics. *J. Stat. Phys.*, 164(4):735–771, 2016.

[23] G. O. Roberts and R. L. Tweedie. Exponential convergence of Langevin distributions and their discrete approximations. *Bernoulli*, 2(4):341–363, 1996.

[24] J. E. Straub, M. Borkovec, and B. J. Berne. Molecular-dynamics study of an isomerizing diatomic in a Lennard-Jones fluid. *J. Chem. Phys.*, 89(8):4833–4847, 1988.

[25] C. R. Sweet, S. S. Hampton, R. D. Skeel, and J. A. Izaguirre. A separable shadow Hamiltonian hybrid Monte Carlo method. *J. Chem. Phys.*, 131(17):174106, 2009.

[26] Z. Trstanova. PhD thesis, 2016.

[27] Z. Trstanova and S. Redon. Estimating the speed-up of Adaptively Restrained Langevin dynamics. *arXiv preprint*, 1607.01489, 2016.

[28] M. Tuckerman. *Statistical Mechanics: Theory and Molecular Simulation*. Oxford University Press, 2010.

[29] L. Verlet. Computer "experiments" on classical fluids. I. Thermodynamical properties of Lennard-Jones molecules. *Phys. Rev.*, 159:98–103, 1967.